Available online at www.sciencedirect.com
SCIENCE DIRECT
Physics and Chemistry of the Earth 31 (2006) 473–481
PHYSICS and CHEMISTRY of the EARTH
www.elsevier.com/locate/pce

Ionospheric plasma response to the seismic activity

H. Rothkaehl [a,*], R. Bucik [a,b], K. Kudela [b]

[a] Space Research Centre, Polish Academy of Sciences, ul. Bartycka 18a, 00-716 Warsaw, Poland
[b] Institute of Experimental Physics, Slovak Academy of Sciences, Košice, Slovakia

Accepted 6 February 2006
Available online 11 May 2006

Abstract

Electromagnetic emissions observed in the nearest earth environment are a superposition of natural emissions and various types of artificial noises. The wave activity detected at the low orbiting satellites can also be a consequence of thunderstorms, earthquakes and volcanic activity. Electromagnetic effects associated with earthquakes have been known for a long time, but no clear explanation of observed facts has been put forward so far. The aim of this paper is to present some selected processes occurring within the ionospheric plasma during seismic activity. The wave measurements detected by the SORS instrument in the 0.1–15 MHz frequency range, as well as the gamma ray fluxes in the energy range 0.12–0.32 and 3.0–8.3 MeV, detected by the SONG instrument, located on the low orbiting satellite CORONAS-I were used to present ionospheric plasma response to the strong seismic activity on 31.03.1994 during quiet geomagnetic conditions and on 6.04.1994 during geomagnetic storm period. In order to better understand the physical conditions and the physical processes in the ionospheric plasma we also presented the character of typical ionospheric parameters registered by a network of ground-based ionosondes.

Keywords: Earthquake; HF electromagnetic emissions; Gamma ray fluxes; Ionospheric disturbances

1. Introduction

Recently many satellite techniques have been used to monitor different types of earthquake-related physical events (e.g. Hayakawa and Molchanov, 2002). The ionosphere and the magnetosphere are modified unintentionally by various types of man-made and cataclysmic events noises. As a consequence, electromagnetic emissions detected by low orbiting satellites are affected by these indicators in broad band frequency range besides certain natural processes in the earth environment.

One of the first events of seismic activity detected in the topside ionosphere by the OGO-6 satellite was electromagnetic emissions registered over the epicentre of an earthquake in Japan (Gokhberg et al., 1983). Furthermore, similar registrations have been performed by AE-C, ISIS-2, AUREOL-3, INTERCOSMOS-19 and COSMOS-1809 satellites. Earthquake-related signals were mainly detected in the ELF–VLF frequency band (Larkina et al., 1989; Chmyrev et al., 1989; Molchanov et al., 1993; Hayakawa et al., 1993; Parrot, 1994; Pulinets and Legen'ka, 1997; Hobara et al., 2005). On the another hand, Galperin et al. (1992), utilising the registration gathered on AUREOL-3 and INTERCOSMOS-BULGARIA 1300 satellites, described the intensification of precipitating high energy electrons and protons with simultaneous excitation of ELF and VLF noises above the earthquake epicentre. Trapped high energy electrons with energy about 1 MeV with anisotropy distribution and hump in the tail were proposed as sources of ELF and VLF signal disturbances. Statistical review of high energy particle flux variation in the inner radiation belts, related to strong earthquakes, was presented by Pustovetov and Malyshev (1992) on the basis of satellite METEOR-3 measurements. The analyses of experimental data gathered by SALYUT-7, INTERCOSMOS-BULGARIA 1300 and METEOR-3 given by

* Corresponding author. Tel.: +48 22 8403766; fax: +48 22 403131.
E-mail address: hrot@cbk.waw.pl (H. Rothkaehl).

1474-7065/$ - see front matter © 2006 Elsevier Ltd. All rights reserved.
doi:10.1016/j.pce.2006.02.039

Galper et al. (1995), Aleksandrin et al. (2001) confirmed appearance of the high energy fluxes associated with seismic activity. The authors indicated that the burst enhancement of high energy fluxes are correlated with seismic activity, and were observed several hours before the earthquake.

The wave and particle diagnostics were also performed by the low orbiting satellite CORONAS-I. Here, parallel to the registration of the plasma emissions in the frequency range 0.1–30 MHz, gamma ray fluxes in the energy range 0.12–0.32 and 3.0–8.3 MeV were gathered. A large variety of observed wave phenomena connected with the changes in the near-earth environment caused by human activity and cataclysmic events were detected (Klos et al., 1997; Rothkaehl et al., 1999). These measurements add a new picture to the scenario of the HF emissions in the topside ionosphere. The aim of this paper is to discuss the responses of high frequency wave activity and high energy particles fluxes to the seismic activity.

2. Instrumentation

CORONAS-I, was launched on March 2, 1994, into the almost near-polar orbit with an altitude of about 500 km and an inclination of 83.0°. This orbit was quasi-synchronous in order to ensure the recurrence of 20-day periods when the orbit was in the Earth's shadow. Aboard the satellite, apart from other instruments, the wave diagnostic instrument SORS and the gamma rays device SONG were located.

The solar radio spectrometer (SORS) was designed to measure radio and plasma noise electric fields. These measurements were performed with a dipole antenna 15 m long from tip-to-tip within the range of 0.1–30 MHz with 25 kHz step and 15 kHz passband. Consecutive spectra were registered every 30 s with a sweep period of 6.4 s each.

The solar neutron and gamma rays (SONG) device consisted of a large area CsI(Tl) scintillator (20×10 cm) surrounded by a 2 cm thick plastic scintillator anticoincidence shield for charged particles. The low energy gamma quanta were measured at four energy release intervals, 0.12–0.32, 0.32–1, 1–3, 3–8.3 MeV with temporal resolution of 2.5 s. The spectrometer had no collimator and its axis was parallel to the longitudinal axis of the satellite.

3. Morphological properties of HF plasma emissions and gamma rays, global distribution

In the topside ionosphere, at the altitude of around 500 km, the properties of ionospheric plasma can be effected by the domination of dense plasma (i.e. where the electron plasma frequency is greater than the electron cyclotron frequency). The analysed HF range covers high frequency whistler waves, Langmuir and upper hybrid modes of the natural plasma emissions. On the other hand, the nonlinear plasma interaction can appear as a wide band turbulent spectrum. Measurements on board CORONAS-I satellite allowed us to detect not only natural plasma emissions, but also, for frequencies greater than local upper hybrid resonance, some artificial noises generated by human activity, e.g. broadcasting station activity (Rothkaehl and Klos, 2003). The properties of natural emissions greatly depend on the conditions of the solar activity, however, the influence of artificial disturbances is very complex and very often related to the wave–particle and wave–wave plasma interaction.

For HF emissions gathered between March–May 1994 and taken into account, the registered spectral intensities were integrated in the frequency range 0.1–15 MHz, in order to produce the average intensity factor. Next this factor was mapped. The well-manifested enhancement of total integrated intensity is visible over certain areas of Europe and a part of Asia. On the other hand, the average intensity factor integrated in frequency range around the local gyrofrequency (in this case up to 2 MHz) can mainly reflect the electron plasma properties at the topside ionosphere (Fig. 1). Those observed enhancements of the mean intensity, in this case, are related to emissions generated by the wave–particle interaction in electron cyclotron and whistler domains. Those investigations show that the maximum of mean HF emissions, in the frequency band around local gyrofrequency, mainly occur during the night time and are related to the radiation belt position.

To illustrate the spatial distribution of precipitating particle fluxes, a global map of gamma rays fluxes in the energy range 0.12–0.32 MeV was constructed (Fig. 2) (Bucik et al., 2000). The irregular distribution of the gamma radiation in the various geographical regions is used to know the radiation belts and SAA structure as well. Gamma rays fluxes observed in the near-earth space experiments are a superposition of atmospheric and local emissions produced in the interaction of primary and secondary cosmic rays, the Van Allen radiation, or interaction of solar cosmic rays with the material of the instrument and the satellite body. Atmospheric gamma rays are produced by interactions of cosmic ray protons, alpha particles, and electrons with oxygen and nitrogen nuclei in the atmosphere. At higher energies, gamma rays are created mainly by the decay of π° mesons from high energy nuclear interactions, while at lower energies the gamma rays are produced primarily by electron Bremsstrahlung.

4. Response of ionospheric plasma to the earthquake

4.1. Quiet geomagnetic condition

In order to present a typical ionospheric response to seismic activity during the lifetime of CORONAS-I mission, two pronounced earthquake events with magnitude larger than 6.0 magnitude have been selected. Using the Earthquake Hazard Program[1] led by the USGS the strong

[1] Earthquake Hazard Program http://neic.usgs.gov/.

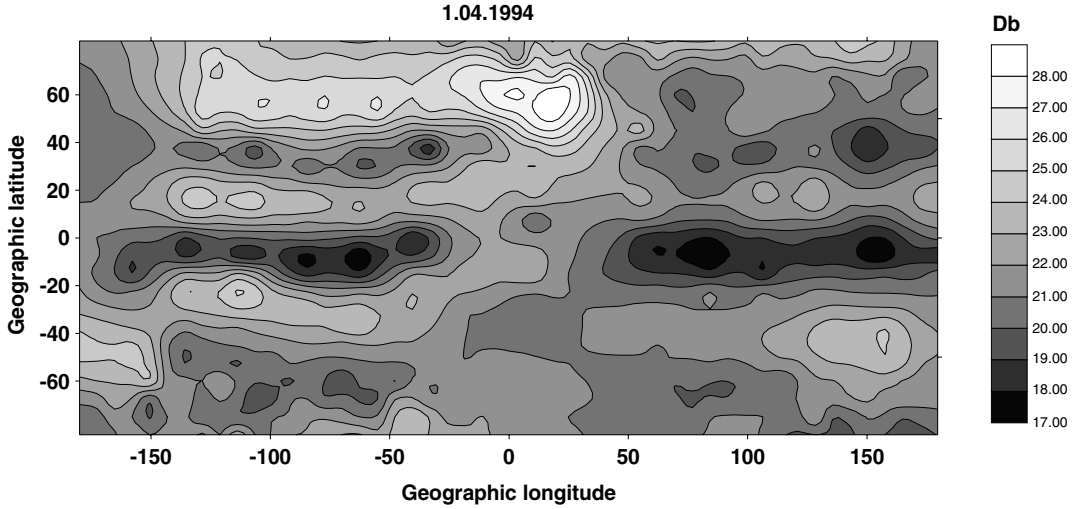

Fig. 1. Global distribution of HF emission in the ionosphere in the frequency range 0.1–2. MHz. The spectral intensity was integrated at various times of day (eastern hemisphere) and night (western hemisphere) 30.03.1994 during quiet condition and recorded by SORS instrument on board the CORONAS-I satellite. The resolution is $5 \times 5°$; the units are DB/μV.

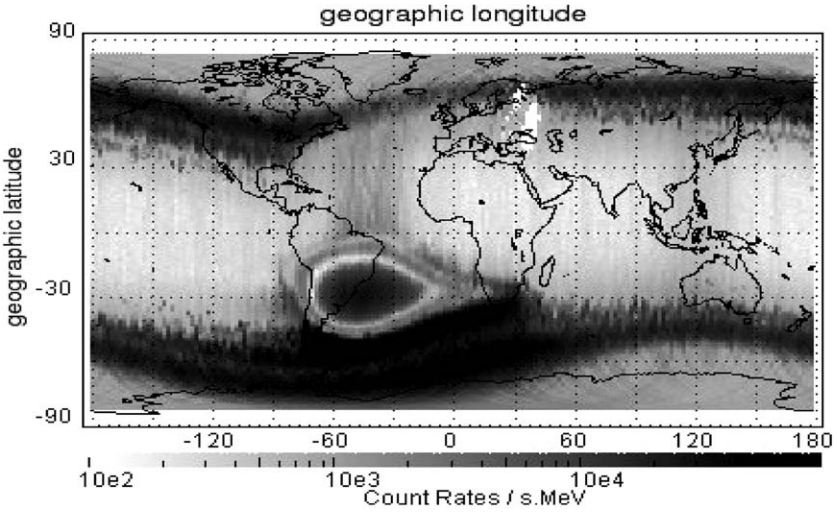

Fig. 2. The map of gamma rays fluxes in the energy range 0.12–0.32 MeV detected by SONG on CORONAS-I satellite during the period from March 1994 through June 1994.

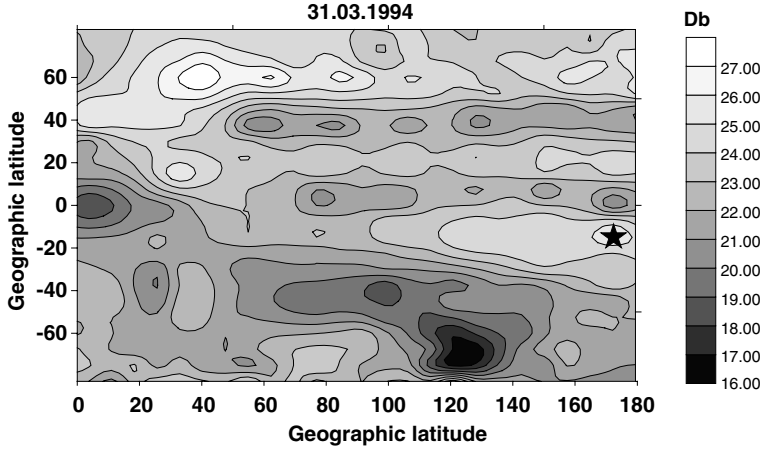

Fig. 3. Global distribution of HF emission in the ionosphere in eastern hemisphere in the frequency range 0.1–2. MHz during. The spectral intensity was integrated at various night times 31.03.1994 quiet condition, recorded by SORS instrument on board the CORONAS-I satellite. The resolution is $5 \times 5°$; the units are DB/μV. The position of maximum HF wave activity is marked by star.

6.5 M earthquake at 22° south geographic latitude and 180° East longitude on 31 March 1994 at 22:41 UT was found. The geomagnetic condition of the Earth environment was stable and very quiet (K_p index was less than 2).

A map of HF noises integrated in the frequency band 0.1–2 MHz has been constructed for the passes of CORONAS-I satellite over the region of seismic activity at the altitude of around 500 km (Fig. 3). The map was constructed during 10 h of satellite passing over the eastern hemisphere. The detected enhancement of HF intensity over the seismic epicentre was registered ten hours before the earthquake. Additionally, the intensification of whistler mode is visible during the next few passes of the spacecraft close to the seismic epicentre area. In similar geomagnetic

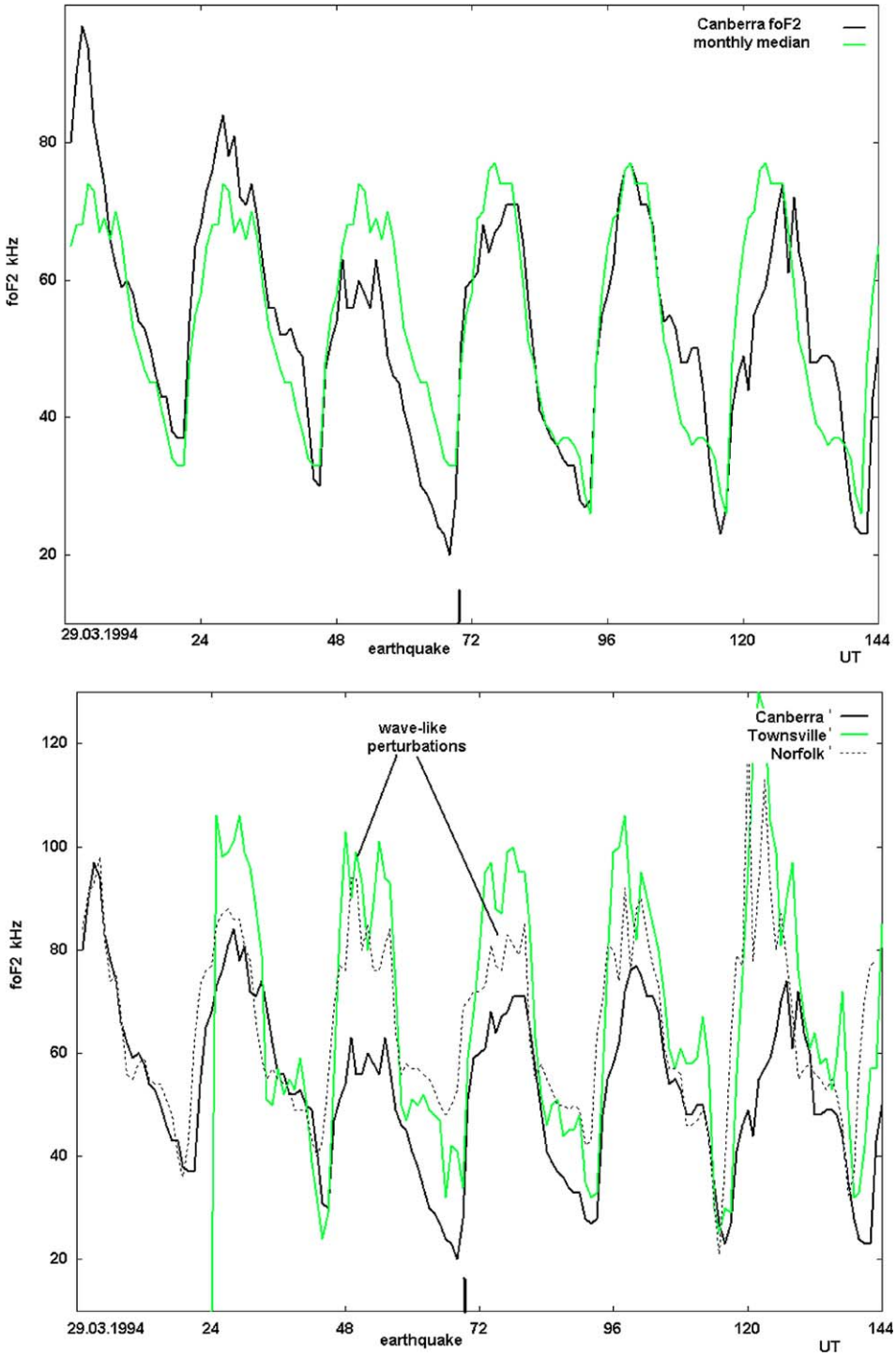

Fig. 4. FoF2 parameter and monthly median for Canberra ionosonde station from 29.03.1994 till 3.04.1994 upper panel, foF2 parameter for Canberra, Townsville and Norfolk station from 29.03.1994 till 3.04.1994 bottom panel. 0 UT responds to 0:0 UT on 29.03.1994. The geomagnetic activity was very low in the period 29.03–02.04.1994 as on 3.04.1994 the beginning of geomagnetic storm was registered.

conditions the wave activity in the whistler frequency range over the area in question was low. The observed maximum of HF emission is registered north-west of the seismic epicentre (18°S; 163°E). The same type of map, but constructed by means of electromagnetic signals integrated from 0.1 to 4 MHz, displays the position of maximum HF emission at the latitude of about 26° south and longitude 150° East. The latter presentation can rather display the pattern of electron density at the satellite altitude, as well as artificial disturbances coming from the ground (the mean electron density in the region under discussion is less than 3 MHz what is equivalent to the electron density about 9×10^4 particle per cm^3 and the local gyrofrequency is less than 1 MHz). In order to display the foF2 variability during seismic activity the data base of ground-based ionosonde network has been investigated. At ground-based ionosonde stations Norfolk (29°S; 168°E), Townsville (20°S; 147°E) and Canberra (35.2°S; 149°E) near the seismic epicentre, significant wave-like changes of foF2 value one day before and one day after the earthquake were detected. The presented data set was registered during the very quiet geomagnetic conditions except the last presented day (3.04.1994) when the beginning of a geomagnetic storm was recorded. The typical period of the observed wave-like perturbation of plasma density at F2 layers is about 1–3 h, which corresponds to the length of the wave-like irregularities of about 350–500 km (Fig. 4). A similar effect was observed and analysed by Fedorenko et al. (2003, 2005) using data gathered on board Atmosphere Explorer-E satellite. The generation of atmospheric gravity waves (AGW) as well as the generation of plasma inhomogeneities of neutral and ionisation plasma component were found in correlation with the occurrence of the strong earthquakes. The disturbances were observed a few thousand kilometers from the earthquake epicenters. A significant drop of the electron density at the maximum F2 layers one day before the earthquake was detected but only in the Canberra station (Fig. 4). The similar effect was observed and described by Hobara and Parrot (2005) using the data from the ionosonde network located near the earthquake epicentres.

The earthquake epicenter was located at the L-shell of 1.3, but the gamma rays measurements indicated the enhancement of fluxes in the 0.12–0.32 MeV at L-shell of 1.56. No significant changes in gamma rays fluxes in the high energy interval between 0.32–1, 1–3, 3–8.3 MeV related to the earthquake were recorded.

In order to better understand the physical properties of scattering electrons and production of gamma rays fluxes, by means of the magnetic field model, the magnetic topology diagram of predicted different sources of gamma rays fluxes at the altitude CORONAS-I spacecraft has been plotted in Fig. 5. A detailed examination shows that the drift loss cone (DLC) electrons are precipitated in the northern hemisphere between 120–180° East and there is also contribution from bounce loss cone electrons (BLC). Finally, at the longitude of 180–230° particles are lost in the atmosphere in the northern hemisphere. If the source of scattering electrons is located over the earthquake (180°) they would mostly precipitate in a stable trapped zone (called SAA). So, as a consequence, we should observe gamma rays fluxes near 180–230° longitude in

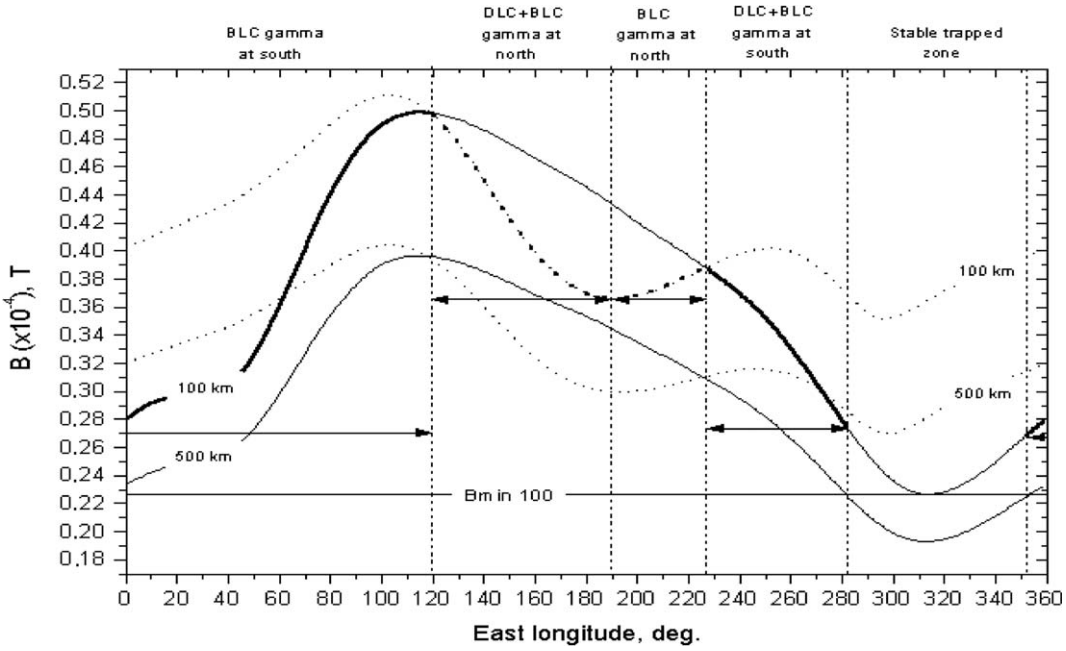

Fig. 5. Magnetic field footprints of L-shell of 1.3 as a function of east longitude at 100 km and 500 km altitudes for Southern (solid) and Northern (dot) hemispheres. Electrons mirroring at $B < B_{min}$ 100 (minimum magnetic field strength at 100 km; indicated by horizontal red line in graph) are stably trapped. Above B_{min} 100, electrons can be in bounce loss cone (BLC) or in the drift loss cone (DLC), depending on the longitude. (For interpretation of the references in colour in this figure legend, the reader is referred to the web version of this article.)

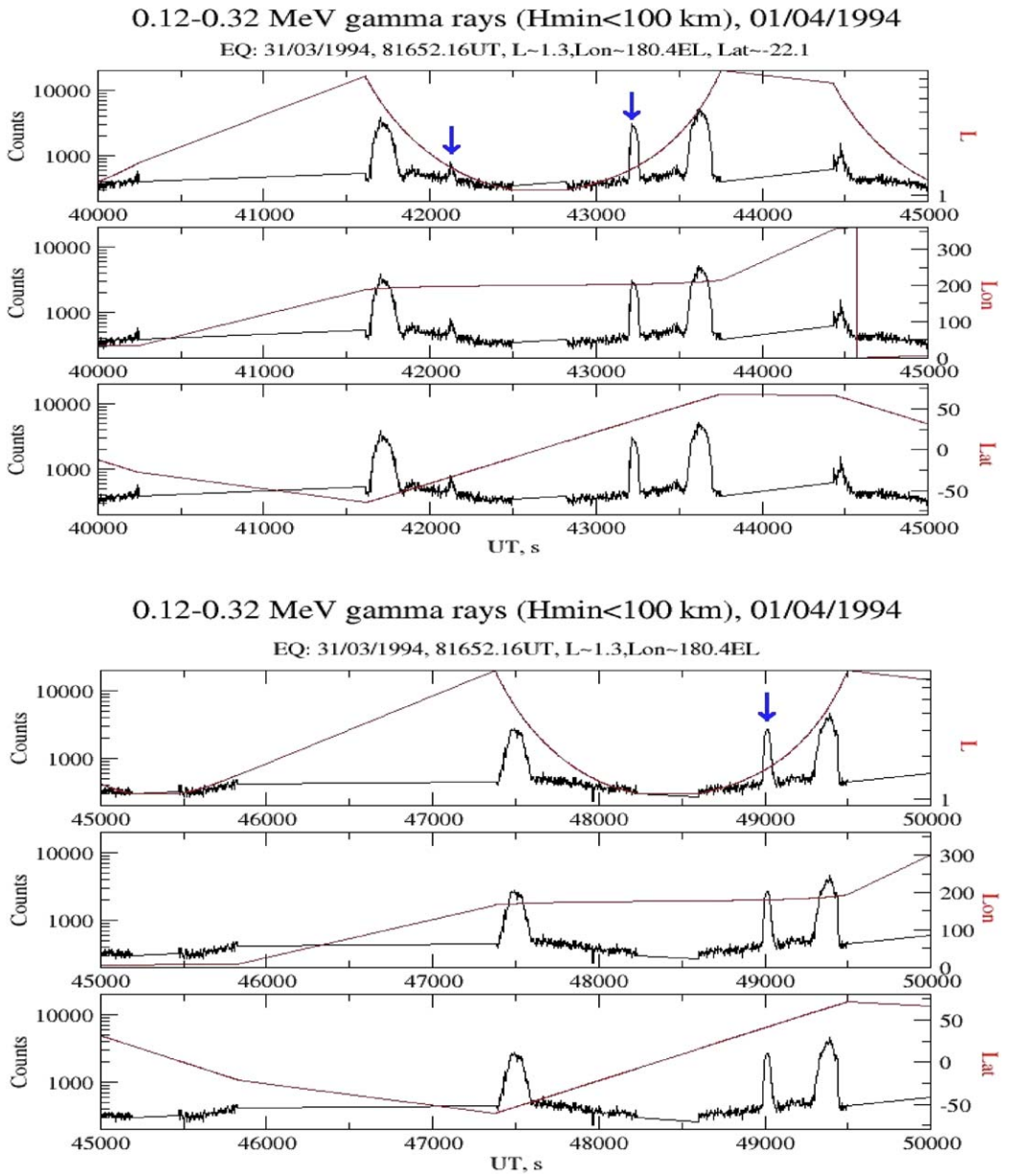

Fig. 6. The gamma ray fluxes in the 0.12–0.32 MeV energy range detected 12 h after main shock of seismic activity. The arrows marked enhancement of BLC electrons fluxes. In the upper panel in the inner radiation belt at L ~ 1.56 two peaks can be seen on the same field line at ~200° on the south at 11:42 UT and on the north at 12:00 UT. In the bottom panel during the next orbit 13:37 UT only northern peak at L ~ 1.65 is visible. The time is calculated in seconds from the beginning of telemetric scans. The earthquake occurs at 81652 s.(22:41 UT). It is also marked the changes of L, Lon geographic longitude and L at geographic latitude during presented time of observation.

the northern hemisphere and weaker fluxes between 230–280 longitude in the southern hemisphere.

The SONG instruments were switched on 12 h after the main shock, nevertheless two peaks at L-shell 1.56 were registered in Fig. 6. As predicted by the model, the northern hemisphere peak is more pronounced. Bounce loss cone (BLC) precipitation is manifested at L ~ 1.56 and at the longitude interval between 180 and 200°. The intensity of the peak decreases with time. Finally, after 12 h, emissions in the southern hemisphere and later on in the northern disappear. One orbit later, drift loss cone (DLC) precipitation at longitudes from 250–280° at the same L-shell was also detected.

4.2. Disturbed geomagnetic condition

The next strong 6.2 M earthquake, but associated with a strong geomagnetic storm, was registered on 6 April 1994 at 12:13 UT at 17° South and 168° East. The map of integrated HF emissions from 0.1 to 2 MHz also indicates slightly (not so pronounce as during quiet geomagnetic conditions) an enhancement of wave intensity, however,

on the map integrated in frequency range 0.1–4 MHz the effect is not noticeable. The satellite was located 4° geographic longitude from the epicenter during the beginning of the earthquake, but passed the region over the earthquake epicenter 1 h 15 min after the main shock. The electromagnetic emissions detected in the ionosphere are influenced by strong wave–particle interaction, therefore the signals of seismic origin are overlapping with the Sun-driven instability. The essential enhancements of HF waves activity in different geographical region driven by increase of the geomagnetic activity are noticeable on the presented global map of electromagnetic noises. On the other hand, fluxes of energetic electrons can generate more intense whistler mode emissions through the Cerenkov mechanism, and as a consequence, even during a geomagnetic storm, the enhancement in the whistler mode, related to the seismic activity can be appreciable as seen in Fig. 7.

The wave analyses allow us to determine the local electron density at the satellite altitude. Those investigations

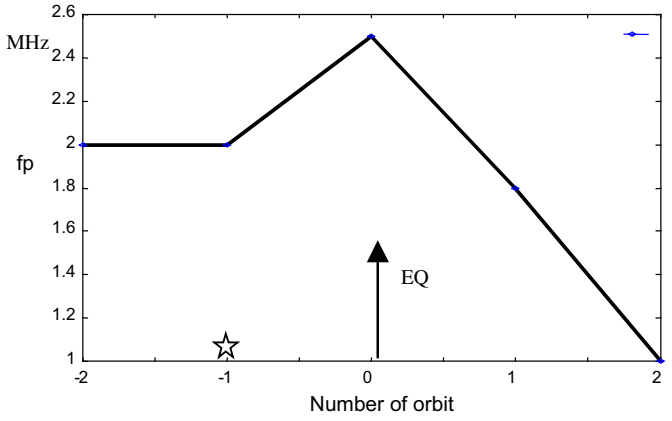

Fig. 8. Local plasma frequency f_p (MHz), proportional to the local electron density, at the satellite altitude (500 km) obtained by the HF wave measurements versus number of or bit (one orbit ca 120 min). The stars marked the time when earthquake occurs, the arrow marked the position of satellite over seismic epicentre 1 h 15 min after earthquake start time.

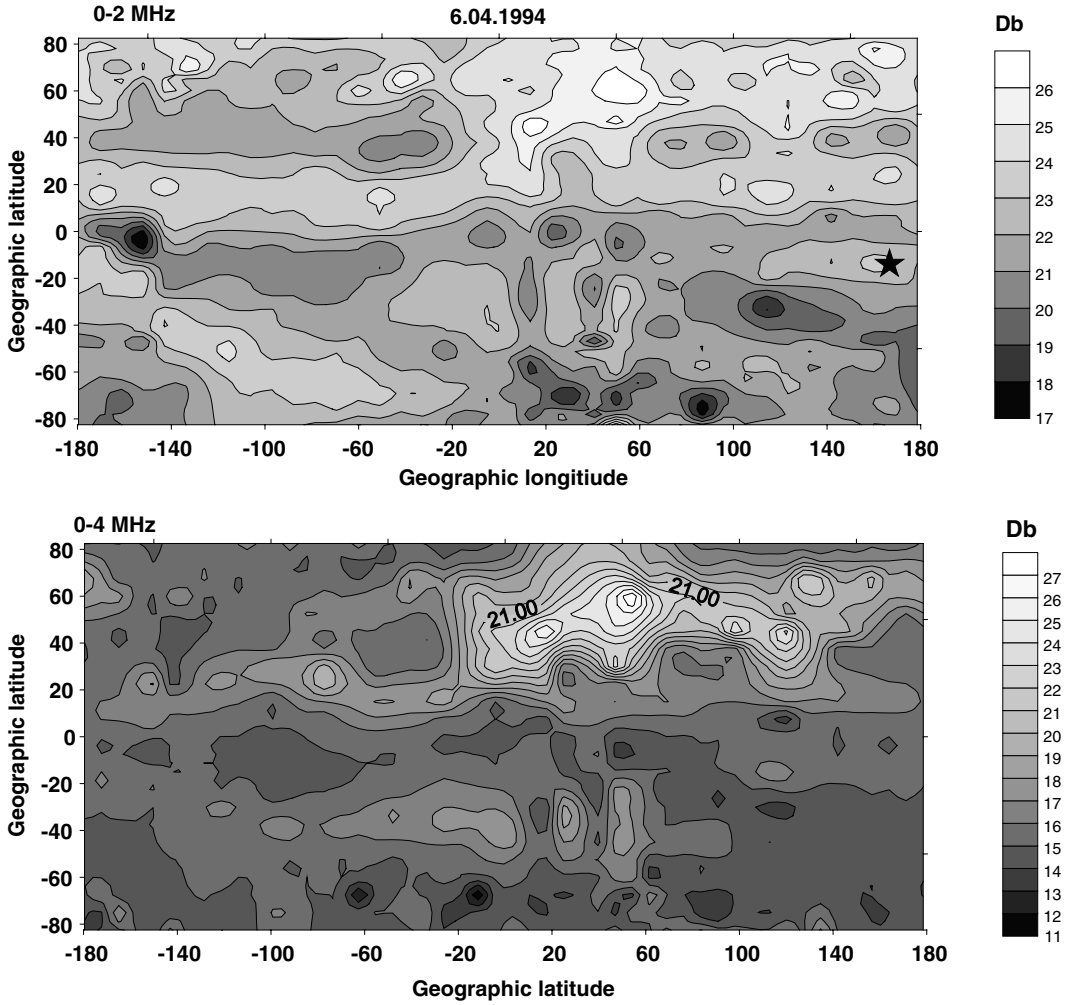

Fig. 7. Global distribution of HF emission in the ionosphere in the frequency range 0.1–2 MHz (upper panel) and 0.1–4 MHz (bottom panel). The spectral intensity was integrated at various times of day and night 6.04.1994 disturbed condition and recorded by SORS instrument on board the CORONAS-I satellite. The resolution is $5 \times 5°$; the units are DB/μV. The epicentre of the earthquake is marked by the star.

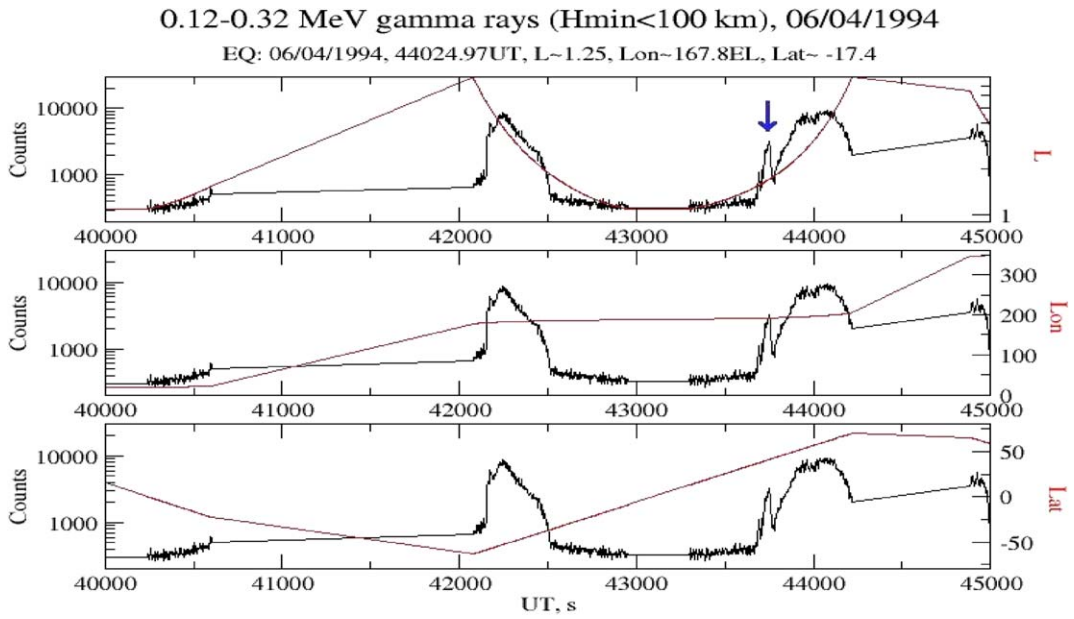

Fig. 9. The gamma ray fluxes in the 0.12–0.32 MeV energy range detected 10 min before the main shock of seismic activity. Blue arrows marked enhancement of bounce loss cone BLC electrons fluxes in northern hemisphere at L ~ 1.65 and at longitude of 190° East. The time is calculated in second from the beginning of telemetric scans. The earthquake occurs at 44025 s.(12:13 UT). Here are marked the changes of L, Lon geographic longitude and Lat geographic latitude during presented time of observation. (For interpretation of the references in colour in this figure caption, the reader is referred to the web version of the article).

indicated the enhancement of electron density in the area of 10° from the seismic epicentre and a few hours before the main shock (see Fig. 8).

On April 6, 1994 the gamma rays measurements show the enhancement of flux at the same L-shell as the seismic epicentre at about 12UT, 10 min before the earthquake in Fig. 9. The detected flux enhancement appeared in the northern hemisphere at L ~ 1.65 and at 190° East. Furthermore both the northern bounce loss cone (BLC) and the southern drift loss cone (DLC) enhancements were observed at L ~ 1.65–1.75. BLC enhancements decreased with time and were detected more than 10 hours later, nevertheless they were still located around 190° East.

5. Conclusion

The magnetosphere–ionosphere–thermosphere subsystem is strongly coupled via the electric field, particle precipitation, heat flows and small-scale interaction. The level of electromagnetic noises detected at the ionospheric altitude depends on properties of geophysical condition, properties of different Earth regions, influences coming from the Earth surface such as cataclysmic events and the satellite and from the surrounding plasma interaction. On the other hand, many observation facts confirmed that the earthquake events can be monitored and detected by the space-borne experiments. The case study of HF wave measurements and gamma rays diagnostic performed on board CORONAS-I satellite show a possible correlation between enhancements of whistler wave activity and soft gamma rays fluxes related to seismic activity. Nevertheless, in the latter presented in this paper, it is more difficult to judge which factor has a greater impact on the generated instability: the Sun-driven or the seismic activity. Upon limited in situ ionospheric plasma observations, enhancements of HF wave activity in whistler mode associated with fluxes of precipitation particles from inner radiation belts during quiet geomagnetic as well as during the disturb condition have been detected. The precipitated fluxes of energetic electrons seem to be a driver of excitation of the HF whistler mode emission, via the Cerenkov incoherent mechanism of generation. The near-Earth plasma environment is very complex and susceptible to change. Parallel to the well-known effects related to the seismic activity in the topside ionosphere such as small-scale irregularities generated due to acoustic waves (Hegai et al., 1997), and large-scale irregularities generated by anomalous electric field (Pulinets et al., 2000), the modifications of magnetic flux tube are also common features (Kim and Hegai, 1997; Pulinets et al., 2002). So it seems that changes of the magnetic flux tube topology correlated with seismic activity can lead to the increase in the precipitation of energetic electron fluxes and, as a consequence, can yield excitation of the HF whistler mode. The proposed process has a cascade-like character. The HF wave and gamma rays diagnostic located on board a low orbiting satellite seem to be good tools besides other instruments for monitoring events associated with the earthquake. But for future examinations we need drastically newly designed instruments with better time and spatial resolution, and ground and space coordinated observation campaign as well.

Acknowledgement

Research partly supported by Polish Committee of Scientific Research Grant No. 78/E-73SPB/COST/T-12/DWM96/2004-2006.

References

Aleksandrin, A., Forzan, F., Galper, A., Grishantseva, L., Koldashov, S., Maslennilov, L., Murashov, A., Picozza, P., Voronov, S., 2001. Origin of high energy charged particle bursts in the near-Earth Space. Procc. ICRC, 4144–4147.

Bucik, R., Kudela, K., Bogomolov, A.V., Myagkova, I.N., Kuznetsov, S.N., Ryumin, S.P., 2000. Distribution of gamma ray fluxes at altitude 500 km CORONAS-I data. Acta Phys. Slovaca 50 (1), 267–274.

Chmyrev, V.M., Isaev, N.S., Bilichenko, S.V., Stanev, G., 1989. Observation by space-borne detectors of electric fields and hydromagnetic waves in the ionosphere over the earthquake centre. Phys. Earth Planet. Int. 57, 110.

Fedorenko, A., Lizunov, G., Rothkaehl, H., 2003. Case study of the upper atmosphere response on strong earthquakes: Satellite and ground base observations, In: Vernon, A. (Ed.), CD Workshop Proceedings, 2nd COST 271 Workshop COST 271 Products for ITU-R and other radiocommunication applications, 2–4 October 2002 Faro, Portugal, RAL, February.

Fedorenko, A., Lizunov, G., Rothkaehl, H., 2005. Satellite observations of wavelike atmosphere perturbations caused bystrong earthquakes. Geomagn. Aeronomy 45 (3), 403–410.

Galper, A.M., Koldashov, S.V., Voronov, S.A., 1995. High energy particle flux variations as the earthquake predictors. Adv. Space Res. 15 (11), 11.131–11.134.

Galperin, Yu.I., Gladyshev, V.A., Jorjio, N.V., Larkina, V.I., Mogilevsky, M.M., 1992. Energetic particles precipitation from he magnetosphere above the epicentre of approaching earthquake. Cosmic Res. 30, 89–106.

Gokhberg, M.B., Philipeinko, V.A., Pokhotelov, O.A., 1983. Seismic precursor in ionosphere. Phys. Solid Earth, Eng Transl. 19, 762.

Hayakawa, M., Molchanov, O.A. (Eds.), 2002. Seismo Electromagnetics: Lithosphere–Atmosphere–Ionosphere Coupling. Terrepub, Tokyo, p. 477.

Hayakawa, M., Yoshino, T., Morgunov, V.A., 1993. On the possible influence of seismic activity on the propagation of magnetospheric whistlers at low latitudes. Phys. Earth Planet Int. 77, 97.

Hegai, V.V., Kim, P., Nikiforova, L.I., 1997. A possible generation mechanism of acoustic gravity waves in the ionosphere. J. Earthquake Predictions Res. 6, 548–589.

Hobara, Y., Parrot, M., 2005. Ionospheric perturbations linked to a very powerful seismic event. J. Atmos. Sol-Terr. Phys. 67, 677–685.

Hobara, Y., Lefeuvre, F., Parrot, M., Molchanov, O.A., 2005. Low-altitude ionopsheric turbulence observed by Aureol-3 satellite. Ann. Geophys. 23, 1259–1270.

Kim, V.P., Hegai, V.V., 1997. On possible changes in the mid-latitude upper ionosphere before earthquake. J. Earthquake Predictions Res. 6, 275–280.

Klos Z., Rothkaehl, H., Zbyszyński, Z., Kuznetsov, S., Grigorian, O., Budko, N.I., Prutensky, I.S., Pulinets, S.A., 1997. The global distribution of HF emission in related to the high energy particle precipitation. In: Sadowski, M., Rothkaehl, H. (Eds.), Plasma 97 Research and applications of plasmas, vol. 1, pp. 395–403.

Larkina, V.I., Migulin, V.V., Molchanov, O.A., Kharkov, I.P., Inchin, A.S., Schvetcova, V.B., 1989. Some statistical resultant on very low frequency radio wave emissions in the upper ionosphere over earthquake zone. Phys. Earth Planet. Int. 57, 100.

Molchanov, O.A., Mazhaeva, O.A., Golivin, A.N., Hayakawa, M., 1993. Observation by Intercosmos 24 satellite of ELF VLF electromagnetic emissions associated with earthquake. Ann. Geophys. 11, 431.

Parrot, M., 1994. Statistical study of ELF/VLF emissions recorded by a low-altitude satellite during seismic events. J. Geophys. Res. 99 (12), 23339–23347.

Pulinets, S.A., Legen'ka, A.D., V.A., 1997. First simultaneous observations of the topside density variations and VLF emissions before Irpinia erarthquake, November 23 1980, In: Proc. of International Workshop on Seismo Electromagnetics, Japan, pp. 56–57.

Pulinets, S.A., Boyarchuk, K.A., Hegai, V.V., Kim, V.P., Lomonosov, A.M., 2000. Quasielectric model of atmosphere–termosphere–ionosphere coupling. Adv. Space Res. 26, 1209–1218.

Pulinets, S.A., Boyarchuk, K.A., Hegai, V.V., Karelin, A.V., 2002. Conception and model of seismo-ionosphere–magnetosphere coupling, Seismo Electromagnetic: Lithosphere–Atmosphere–Ionosphere coupling In: Hayakawa, M., Molchanov, O.A. (Ed.), pp. 353–361.

Pustovetov, V.P., Malyshev, A.B., 1992. Space–time correlation of earthquake and high energy particle flux variations in the inner radiation belts. Cosmic Res. 31, 8490.

Rothkaehl, H., Klos, Z., 2003. Broadband HF emissions as an indicator of global changes within ionosphere. Adv. Space Res. 31 (5), 1371–1376.

Rothkaehl, H., Klos, Z., Zbyszyński, Z., Kuznietsov, S., Grigorian, O., Gotseljuk, Budko, N.I., Prutensky, I.S., Pulinets, S.A., 1999. The global distribution of RF emission in the topside ionosphere and high energy particle precipitation. In: Infeld, E., Rothkaehl, H., Sadowski, M. (Eds.), J. Tech. Phys. 40, pp. 313–316.